

We have recently developed a novel inorganic/organic nanocomposite for a soft-tissue-compatible material: a flexible silicone elastomer [6] or a silk fibroin [7], whose surface was modified with calcined HAp crystals through covalent bonding. The novel composite retained the flexibility of the polymer substrate and showed good tissue adhesion due to the HAp crystals on the surface [8]. Throughout these studies, the HAp crystals were used after calcination at 800°C to reduce *in vivo* sorbability. As mentioned above, the HAp nanoparticles mostly sintered into large agglomerates of polycrystals during calcination. This made it difficult to control the surface coverage of the composite by HAp crystals and the roughness of the composite surface.

Hydrothermal treatment of HAp particles in water medium under high pressure is known to enable the preparation of agglomerate-free HAp crystals [9-11]. However, this treatment generally leads to an increase in crystal size due to Ostwald ripening [12, 13], and is restricted to laboratory-scale products as it is a high-pressure process.

The present study reports the preparation of nano-sized, calcinated HAp single crystals protected against calcination-induced sintering using an anti-sintering agent interspersed between the HAp particles. Thus, there was no contact between the particles during calcination. Calcium hydroxide [Ca(OH)<sub>2</sub>] was selected as an anti-sintering agent because it would not melt at the calcination temperature (800°C), presumably not dissolve the HAp, and could be removed by washing with water after calcination.

Starting HAp particles with low crystallinity were prepared by a modified emulsion system at 25°C [14]. The resulting product was centrifugally washed and redispersed in water (solid content: 5 wt%). In order to intersperse Ca(OH)<sub>2</sub> between the particles, the HAp aqueous dispersion was added into a saturated aqueous Ca(OH)<sub>2</sub> solution (0.17 wt%), and the mixture was dried under reduced pressure at 40°C. The resultant HAp/Ca(OH)<sub>2</sub> (1/1, w/w) mixture was calcined at 800°C for 1 h in air (heating rate: 10°C/min). After calcination, the

mixture was centrifugally washed with a 10 mM aqueous ammonium nitrate solution to remove the  $\text{Ca}(\text{OH})_2$ . As a control, some HAp was calcined using the same procedure, but without adding  $\text{Ca}(\text{OH})_2$ . The HAp crystals were observed by scanning electron microscopy (SEM; JSM-6301F, JEOL Ltd., Tokyo, Japan) and transmission electron microscopy (TEM; JEM-2000 EXII, JEOL Ltd.). Size distribution of the HAp crystals dispersed in ethanol was measured at 10-ppm concentration by dynamic light scattering (DLS) (ELS-8000, Otsuka Electronics Co., Ltd., Kyoto, Japan) at a light-scattering angle of  $90^\circ$ .

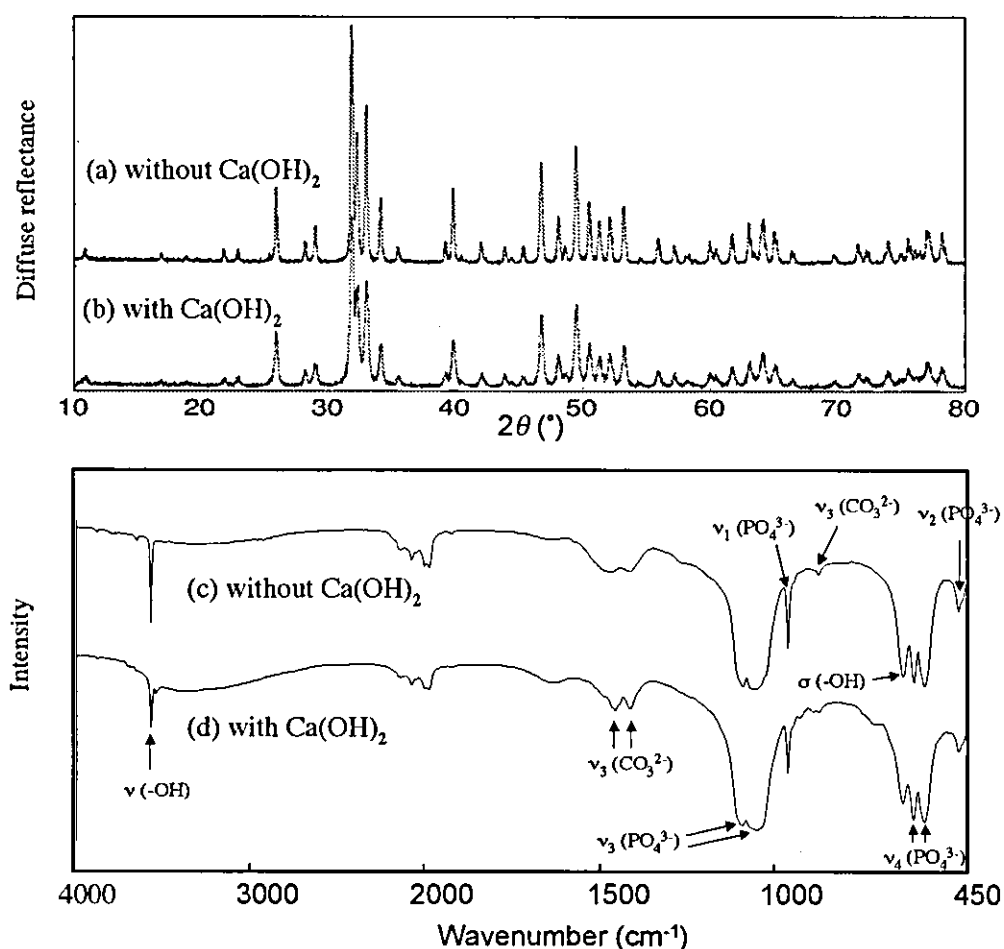


Fig. 1 X-ray diffraction patterns (a, b) and FTIR spectra (c, d) of hydroxyapatite (HAp) particles calcined at  $800^\circ\text{C}$  for 1 h without (a, c) and with (b, d)  $\text{Ca}(\text{OH})_2$  ( $\text{HAp}/\text{Ca}(\text{OH})_2 = 1/1$  w/w) interspersed between the particles.  $\text{Ca}(\text{OH})_2$  was centrifugally washed off with an aqueous solution after calcination.

In order to examine the effect of  $\text{Ca(OH)}_2$  on the crystal phase and composition of HAp, X-ray diffraction (XRD; RAD-X, Rigaku International Co., Tokyo, Japan) with  $\text{CuK}\alpha$  radiation and Fourier-transform infrared (FTIR) spectroscopy (Spectrum One, Perkin-Elmer Inc., MA, USA) were performed. The results are shown in Fig. 1. In Figs. 1(a) and (b), both XRD profiles showed highly crystalline HAp, and no other calcium phosphate phases could be detected. In the FTIR spectrum of HAp calcined with  $\text{Ca(OH)}_2$  (Fig. 1(d)), no peaks due to stretching of OH in  $\text{Ca(OH)}_2$  were observed at  $3640\text{ cm}^{-1}$ , indicating complete removal of  $\text{Ca(OH)}_2$ . Bonel *et al.* prepared calcium-rich apatites with a Ca/P molar ratio above 1.67 by heating a mixture of stoichiometric HAp [ $\text{Ca}_{10}(\text{PO}_4)_6(\text{OH})_2$ ; Ca/P = 1.67] and  $\text{CaCO}_3$  in moist air at  $1000^\circ\text{C}$  for 10 days, and identified additional OH IR bands at 3544, 745, 715, and  $680\text{ cm}^{-1}$  [15]. In the present study, although the additional band at  $3544\text{ cm}^{-1}$  was observed, the Ca/P ratio of the HAp calcined with  $\text{Ca(OH)}_2$  was 1.58 (1.56 in the case of the HAp calcined without  $\text{Ca(OH)}_2$ ). These results suggest that calcination with  $\text{Ca(OH)}_2$  led to the formation of a calcium-rich apatite phase only on the outermost surface, presumably because the conditions (temperature, time, composition of atmosphere) were too mild for a reaction between HAp and  $\text{Ca(OH)}_2$ . It is worth pointing out that the calcium-rich carbonate-substituted HAp had improved mechanical and biological properties compared to stoichiometric HAp [16].

Fig. 2 shows SEM and TEM micrographs of HAp crystals calcined with or without  $\text{Ca(OH)}_2$  and their size distribution measured in ethanol as a medium. As seen in the lower magnification images in Figs. 2 (a) and (b), the crystal size ranged from 30 to 80 nm, irrespective of the presence or absence of  $\text{Ca(OH)}_2$ . The higher magnification TEM image of a particle calcined with  $\text{Ca(OH)}_2$  and its electron diffraction pattern (Figs. 2 (c) and (d), respectively) confirmed that the particle was a single HAp crystal with an irregular spherical morphology. The size of HAp crystals dispersed in ethanol was measured by DLS (Figs. 2 (e)

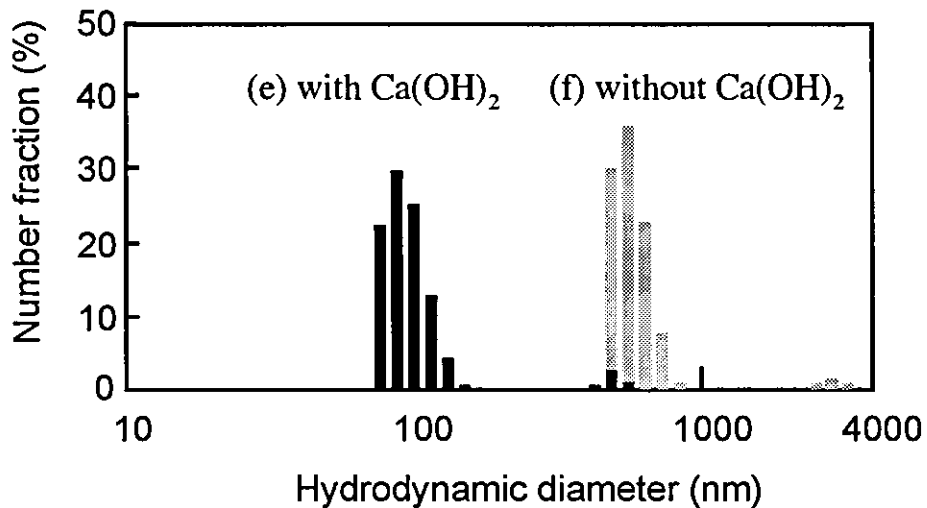
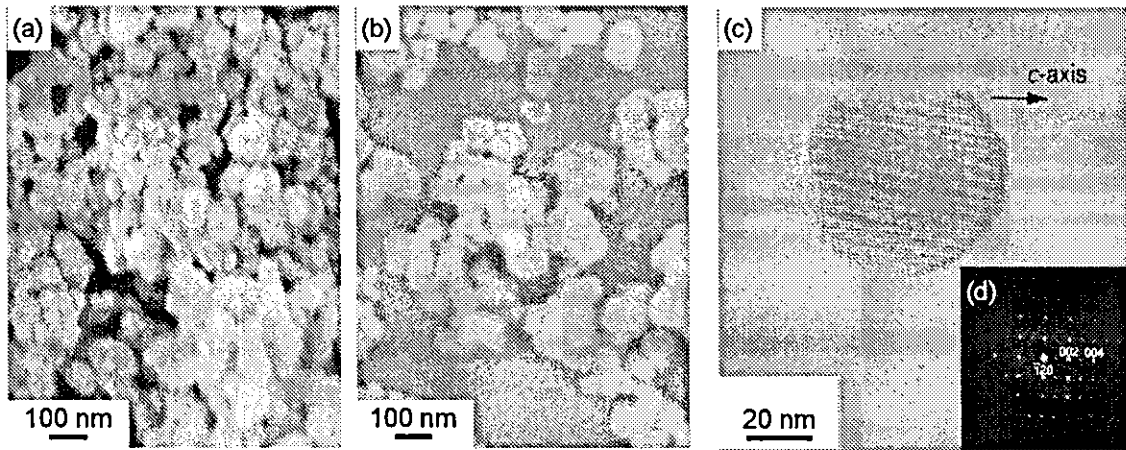


Fig. 2 SEM photographs (a, b) of HAp crystals calcined without (a) and with (b)  $\text{Ca}(\text{OH})_2$ . A TEM photograph (c) and the associated electron diffraction pattern corresponding to the [210] zone (d) of a HAp crystal calcined with  $\text{Ca}(\text{OH})_2$ , showing the crystal to consist of a single HAp phase. Size distributions of HAp crystals calcined without (e) and with (f)  $\text{Ca}(\text{OH})_2$ . The size distributions were measured in ethanol.

and (f)). In the case of calcination without  $\text{Ca}(\text{OH})_2$ , the mean size was about 600 nm, which indicates the formation of agglomerates of sintered HAp polycrystals. In the case of calcination with  $\text{Ca}(\text{OH})_2$ , the size of particles dispersed in ethanol ranged from 80 to 130 nm, which is close to the primary crystallite size (30 to 80 nm) determined by electron micrographs. This indicates that sintering between the HAp nanocrystals can be mostly prevented by interspersing  $\text{Ca}(\text{OH})_2$  between the crystals prior to calcination.

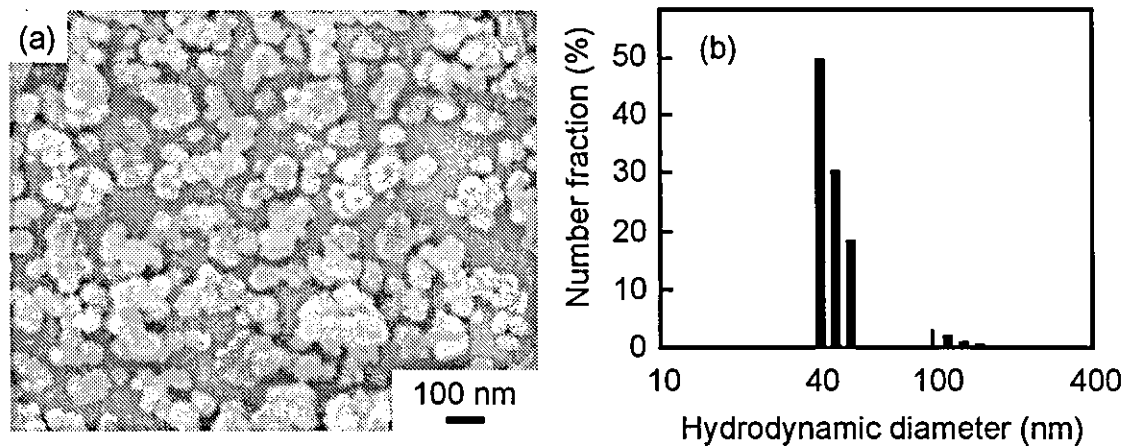


Fig. 3 A SEM photograph (a) and the size distribution (b) of HAp crystals calcined at 800°C for 1 h with poly(acrylic acid calcium salt) (PAA-Ca) surrounding the particles. CaO, the product of thermal decomposition of PAA-Ca, was centrifugally washed off with an aqueous solution after calcination.

However, the size of the dispersed crystals was slightly larger than that of the primary particles. This is should be because HAp particles have both anionic and cationic surfaces, and hence, tend to flocculate in aqueous media. The particle size measurements indicate that these agglomerates that formed during interspersions of the  $\text{Ca}(\text{OH})_2$  contained several HAp particles each. Thus, poly(acrylic acid) (PAA) was added as a deflocculant before the addition of  $\text{Ca}(\text{OH})_2$ . PAA can adsorb on the HAp surfaces [17, 18], and thus, act as a polymeric dispersant. The addition of calcium ions into an aqueous PAA solution induces a rapid precipitation of poly(acrylic acid calcium salt) (PAA-Ca). Thus, when calcium ions are added to the PAA-stabilized HAp dispersion, PAA-Ca precipitates onto the surface of the HAp particles, and presumably acts as an anti-sintering agent. In the present study, an amount of PAA (Sigma-Aldrich Co.; weight-average molecular weight: 15,000), approximately equal in weight to the HAp particles, was added under alkaline conditions (initial pH: 10). An excess amount of calcium ions were added to the dispersion in the form of a saturated aqueous  $\text{Ca}(\text{OH})_2$  solution ( $\text{Ca}(\text{OH})_2/\text{COOH}$  in PAA = 1/1 molar ratio). The resultant HAp/PAA-Ca

mixture was calcined in the manner described above, and then washed to remove CaO, the product of thermal decomposition of PAA-Ca. The resultant HAp crystals are shown in Fig. 3. The size of the HAp crystals dispersed in ethanol (40 to 70 nm) corresponded to that of the primary crystallites (30 to 80 nm), which indicates that HAp nanocrystals calcined with PAA-Ca can be dispersed as single crystals. IR spectrum and XRD pattern of the HAp single crystals calcined with PAA-Ca were the same as those shown in Figs. 1(b) and (d). The achieved high dispersibility of HAp single crystals appears to be due to either the crystals' irregular shape, that is, the absence of specific anionic or cationic surfaces, or the cationic charge of the outermost calcium-rich surface.

In summary, calcined HAp nanocrystals were successfully prepared by calcination using an anti-sintering agent interspersed between or surrounding the particles, followed by removal of the agent. The HAp nanocrystals obtained here should be suitable for the various applications mentioned above, and also as dental and orthopedic ultrafine fillers for microporosity owing to their high dispersibility in liquid media and high thermal and chemical stability. Furthermore, calcination with an anti-sintering agent should be applicable to the production of calcined nanoparticles of other materials, such as alumina and titania.

### **Acknowledgments**

We thank Dr. K. Sato of Ceramic Research Institute, AIST, for helpful discussions. This work was partially supported by grants from PRESTO, Japan Science and Technology Agency, and the Ministry of Health, Labour and Welfare of Japan.

## References

1. J. Frenkel, *J. Phys.* **1945**, *9*, 385
2. G. C. Kuczynski, *Trans. AIME* **1949**, *185*, 169
3. J. E. Barralet, S. M. Best, W. Bonfield, *J. Mat. Sci.: Mater. Med.* **2000**, *11*, 719
4. E. Landi, A. Tampieri, G. Celotti, S. Sprio, *J. Eur. Ceram. Soc.* **2000**, *20*, 2377
5. D. Bernache-Assollant, A. Ababoua, E. Championa, M. Heughebaertb, *J. Eur. Ceram. Soc.* **2003**, *23*, 229
6. T. Furuzono, K. Sonoda, J. Tanaka, *J. Biomed. Mater. Res.* **2001**, *56*, 9
7. T. Furuzono, A. Kishida, J. Tanaka, *J. Mater. Sci.: Mater. Med.* **2004**, *15*, 19
8. T. Furuzono, P. Wang, A. Korematsu, K. Miyazaki, M. Oido-Mori, Y. Kowashi, K. Ohura, J. Tanaka, A. Kishida, *J. Biomed. Mater. Res. B: Appl. Biomater.* **2003**, *65B*, 217
9. S. Somiya, K. Ioku, M. Yoshimura, *Mater. Sci. Forum JST.* **1988**, *34/36*, 371
10. M. Yoshimura, H. Suda, K. Okamoto, K. Ioku, *J. Mater. Sci.* **1994**, *29*, 3399
11. A. D. Papargyris, A. I. Botis, S. A. Papargyri *Key Eng. Mater.* **2002**, *206/213*, 83
12. J. E. Carless, A. A. Foster, *J. Pharmaceut. Pharmacol.* **1966**, *18*, 697
13. M. Wei, A. J. Ruys, B. K. Milthorpe, C. C. Sorrell, *J. Biomed. Mater. Res.* **1999**, *45*, 11
14. T. Furuzono, D. Walsh, K. Sato, K. Sonoda, J. Tanaka, *J. Mater. Sci. Lett.* **2001**, *20*, 111
15. G. Bonel, J.-C. Heughebaert, M. Heughebaert, J. L. Lacout, A. Lebugle, *Ann. N.Y. Acad. Sci.* **1988**, *523*, 115
16. I. R. Gibson, W. Bonfield, *J. Biomed. Mater. Res.* **2002**, *59*, 697
17. D. N. Misra, *J. Dent. Res.* **1993**, *10*, 1418
18. Y. Yoshida, B. Van Meerbeek, Y. Nakayama, M. Yoshioka, J. Snauwaert, Y. Abe, P. Lambrechts, G. Vanherle, M. Okazaki, *J. Dent. Res.* **2001**, *80*, 1565

**Improvement of cell adhesiveness of poly(ethylene terephthalate) by surface modification with hydroxyapatite nanocrystals through covalent bonding**

Miwa Masuda<sup>1</sup>, Masahiro Okada<sup>1</sup>, Shoji Yasuda<sup>1</sup>, Hiroyuki Kadono<sup>2</sup>, Ryoichi Tanaka<sup>3</sup>, Takashi Inenaga<sup>4</sup>, Kunio Miyatake<sup>5</sup>, and Tsutomu Furuzono<sup>1\*</sup>

<sup>1</sup>Department of Biomedical Engineering, Advanced Medical Engineering Center, National Cardiovascular Center, 5-7-1 Fujishirodai, Suita, Osaka 565-8565, Japan

<sup>2</sup>veterinary Surgical Center, 1-6-45 nakahozumi, Ibaraki, Osaka 567-0034, Japan

<sup>3</sup>Department of Radiology, National Cardiovascular Center, 5-7-1 Fujishirodai, Suita, Osaka 565-8565, Japan

<sup>4</sup>Departm

<sup>5</sup>National Cardiovascular Center, 5-7-1 Fujishirodai, Suita, Osaka 565-8565, Japan

\*Author to whom all correspondence should be addressed at Department of Biomedical Engineering, Advanced Medical Engineering Center, National Cardiovascular Center 5-7-1 Fujishirodai, Suita, Osaka 565-8565, Japan

Tel: +81-6-6833-5012 (ext 2623)

Fax: +81-6-6872-7485

E-mail: furuzono@ri.ncvc.go.jp



## **Abstract**

A novel composite of poly(ethylene terephthalate) (PET) fabric, the surface of which was modified with nano-sized hydroxyapatite (HAp) crystals through covalent bonding was developed for a soft-tissue-compatible material. In order to make covalent bonding between the HAp crystal and the PET surface, poly( $\gamma$ -methacryloxypropyl triethoxysilane) [poly(MPTS)] was grafted on the PET surface. The surface grafting of poly(MPTS) onto the PET surface was confirmed by the weight gaining and X-ray photoelectron spectroscopy. The chemical reaction between OH groups on the HAp crystals and ethoxysilyl groups on the poly(MPTS)-grafted PET was conducted at 80\_C for 2h in reduced pressure. The HAp/PET composite was not toxic for human umbilical vein endothelial cells (HUVEC), and HUVEC adhered more plentifully on HAp/PET composite than untreated PET or hydrolyzed poly (MPTS)-grafted PET after 4 h of incubation.

**Key words** Composite • human umbilical vein endothelial cells • poly(ethylene terephthalate)

## Introduction

Such unique biological properties are favorable for soft tissue to closely adhere to Hydroxyapatite (HAp) surface. HAp has unique properties for biomaterials such as hard-tissue-compatible material for bone and tooth [1] and also soft-tissue-compatible material for skin tissue [2]. From the point of view of soft-tissue-compatible material made up of HAp, although the reasons for the compatibility have not been manifested completely, one of them might be favorable to adsorption of adhesion molecules or growth factors *in vivo* on the HAp surface [3]. It is known that HAp is especially efficient at absorbing many proteins in serum *in vivo*. Adhesion proteins in an extracellular matrix, such as fibronectin and vitronectin are actually adsorbed abundantly on the surface of sintered HAp disks compared with titanium or steel. Carbonated HAp could also play a role as a potential carrier of basic fibroblast growth factors (bFGFs), which are potent angiogenic elements having a crucial function in wound-healing processes.

Many artificial organs and devices, such as ventricular assist devices, peritoneal dialysis catheters, blood-access tubes, and intragastric nutrition devices, are implanted percutaneously *in vivo* through the skin.

Sintered HAp, however, possesses the faults of all ceramics, the nature of which is hard and brittle. There is also the fact that a ceramic disk as a percutaneous device installed in a catheter could prevent adequate movement in some patients and cause discomfort as a result of its rigid and solid form. To overcome this problem, a novel inorganic-organic composite consisting of micro or nano-scaled HAp particles and polymer substrate via a covalent linkage has been designed.

An unique composite of sintered HAp micro-particles covalently coupled to silicone and silk fibroin elastomer as soft tissue-compatible material was developed recently [5,6]. The HAp particles were attached to the silicone and silk fibroin substrate covalently without damaging the mechanical properties of the polymer substrate. In this way, the adhesion strength between the HAp particles and polymer substrate, however, was believed to be unsatisfactory because a commercial grade of a HAp spherical particle with an average diameter of 2.0  $\mu\text{m}$  was used. To increase the interaction between the HAp particles and polymer substrate surface, a nano-scaled HAp particle with a large surface area of adhesion on a polymer substrate has been developed by an emulsion system [7,8]. It is expected that the inorganic-organic composite can be satisfactorily developed using the nano-scaled HAp particle and poly(ethylene terephthalate) (PET) fabric as a polymer substrate through covalent linkage. Chemical modification of PET by graft polymerization has been studied by many authors. A factor that may effect the grafting reaction is pretreatment of the fiber or film before the reaction is allowed to commence these pretreatments have been primarily treatment with swelling solvents. A preswelled polymer is more easily grafted than one that has not been swelled. However activation mechanism on PET fabric surface is not practically studied.

## **Materials and methods**

### **Materials**

PET fabric (NBC Inc., Tokyo, Japan) was cleaned by soxhlet extraction with methanol for 24 h to remove any material adhering on the surface, rinsed with distilled

water, and dried at 60°C for 24 h.  $\gamma$ -Methacryloxypropyl triethoxysilane (MPTS) was donated by (Shin-Etsu Chemical Industries Co. Tokyo, Japan). Benzyl alcohol (guaranteed reagent; Nakarai Teque Inc, Kyoto, Japan), methanol (superior quality of reagent; WAKO, pure chemical, Osaka, Japan), H<sub>2</sub>O<sub>2</sub> (superior quality of reagent; SIGMA, Tokyo, Japan) was used as received. Nano-scaled HAp particles were prepared by an alternating emulsion system using calcium hydroxide and potassium dihydrogen phosphate and subsequently sintered at 80°C for 1 h, as described in previous articles [3].

### **Graft Polymerization Procedure**

Unless otherwise indicated, the graft polymerization was carried out as follows: PET fabric was carefully immersed in a 0.2N aqueous NaOH solution for 30 min at 60°C. Then, the hydrolyzed fabric was rinsed with Milli-Q water, which led to carboxylate-functionalized surface [10]. Carboxylate-functionalized PET fabric (0.03g) was introduced into in a 100 ml flask equipped with an inlet of N<sub>2</sub>, a reflux condenser, and a stirrer, and then purged with N<sub>2</sub> for 30min. 45 ml of benzylalcohol containing MPTS (10 wt%) was added in the flask and further purged with N<sub>2</sub> for 30 min at 85°C. After that, 785 $\mu$ l of H<sub>2</sub>O<sub>2</sub> (100 meq/L) used as an initiator was added, and the content was stirred occasionally during the polymerization. After the graft polymerization for a certain period, the PET fabric was washed with ethanol several times to stop the polymerization and to remove homopolymer formed during the polymerization, and dried under reduced pressure for 30 min at 70°C until the weight of fabric was not changed. Weight gain after the polymerization was calculated from the following equation:

$$\text{Weight gain (wt\%)} = (W_2 - W_1) / W_1 \times 100$$

Where  $W_1$  and  $W_2$  are the dried original PET and poly(MPTS)-grafted PET, respectively.

### **HAp/PET composite**

After the HAp particles were suspended in ethanol as a solvent, the poly(MPTS)-grafted PET fabric was soaked in the suspension for 1 h at room temperature. The poly(MPTS)-grafted PET fabric with adsorbed HAp particles was washed by stirring in ethanol, and heated at 80°C for 2 h under in vacuum (1 mmHg) for the reaction between OH groups on the HAp crystals and ethoxysilyl groups on the poly(MPTS)-grafted PET. The composite was washed in ethanol using an ultrasonic generator for 1 min (output: 20 kHz and 35W) to remove unreacted HAp particles attached to other particles in ethanol. Finally, the composite was washed in a great amount of distilled water for 1 day to remove the residual organic solvents used in the synthesis process.

### **Surface analysis**

To characterize the surface-modified samples, and X-ray photoelectron spectroscopy (PHI Inc. 1600S type, Tokyo, Japan). HAp particles in the HAp/PET composite as well as its cell morphology was observed by a 5-KV scanning electron microscopy (SEM; JSM-6301F, JEOL, Tokyo, Japan).

### **Cell adhesion**

Human umbilical vein endothelial cells (HUVEC) were cultured in Endothelial cell basal medium-2 (EGM-2) in air containing 5 % CO<sub>2</sub> in at 37°C. HUVEC were plated onto the HAp/PET composite fabric in 24-well multiplates at 1 x 10<sup>5</sup> cells/ml in EGM-2 and, incubated at 37°C for 4 h. After the fabric was washed twice in phosphate-buffered saline [PBS (-)]. The number of cells was counted with a hemacytometer.

After trypsinization and dilution cells adhering on the fabric was observed by SEM. Samples for SEM observation were prepared as follows. After being rinsed with PBS (-), Huvec adhering on the fabric were fixed with 2.5 % buffered-glutaraldehyde for 20 min at room temperature. Cells were dehydrated step by step with aqueous ethanol (50-100%) and 100% *n*-butanol for 5 min at room temperature step by step.

Nuclear of HUVEC on the fabric was stained with Hoechst33342 (1 μM, Calbiochem, Tokyo, Japan) [12], and observed by fluorescence microscopy (Nikon Tokyo, Japan). 5% collagen-coated PET fabric was used as a positive control.

## **Result and Discussion**

### **Graft polymerization of MPTS on PET fabric**

In order to make covalent bonding between the HAp crystal and the PET fabric, graft polymerization of MPTS on the PET fabric was conducted according to the literature [11]. MPTS has alkoxy-silyl groups which can be coupled with OH groups on HAp surfaces [?]. Figure 1 shows the influence of polymerization time at 85°C on the weight gain of the PET fabric. The weight gain of the PET fabric increased with an increase in the polymerization time, and reached a plateau value of about 4 wt% after 2 h. A Hebeish et

al [1] demonstrated the poly(acrylic acid)-grafted PET having 3.8wt% of weight gain against intact PET. As both obtained results close, Using H<sub>2</sub>O<sub>2</sub> as initiator was not indeed problem.

In order to confirm the grafting of poly(MPTS), XPS measurements were conducted for the untreated PET and that after the polymerization for 2 h. Figure 2 shows the results a peak due to Si was observed in the case of the PET fabric after the polymerization. In the following experiments, 4wt% of weight gain against intact PET was used.

### **HAp/PET composite**

Figure 3 shows a SEM photograph of a HAp-coated PET fiber. In the case of the ungrafted PET, HAp particles were rarely observed on the surfaces because the nanoparticles separated or aggregated with several crystals, meanwhile, strongly remained on the treated PET surface, though some larger aggregates were removed by shear stress using an ultrasonic generator. A HAp crystal has two planes-the a- and c-plane. It is well known that the a-and-c plane show cationic and anionic charge, respectively [7]. We are now examining the adsorption behavior using a quartz crystal microbalance technique. Ionic charge of the HAp surface, moreover, might complexly influence against its bioactivity.

### **Cell adhesion**

To evaluate cell adhesiveness on the HAp/PET composite, the morphologies of HUVEC incubated on sample fabric was observed by SEM and fluorescent microscopy. Figure 4

shows nuclei of HUVEC stained by fluorescence dye on sample substrates after 4 h of incubation. 5% collagen-coated PET fabric was used as a positive control. It was found that cells adhered to HAp/PET as a monolayer as well as collagen-coated PET, the positive-control substrate, because nuclei separated in fluorescence photographs. P. Hamerli et al. [6] obtained results close to ours. The cells hardly adhered to the hydrolyzed poly(MPTS)-grafted PET or untreated PET. In fluorescent photographs of nuclei stained with Hoechst 33342. Prior to cell adhesion, it is believed that cell adhesion protein in serum, such as fibronectin, vitronectin, and bFGF, absorb onto the HAp surface much better than onto the area of dehydrated graft polymer. A similar phenomenon is expected to take place at the interface between a cell and a HAp composite on a nano-scaled HAp/PET composite substrate. That is to say, sintered HAp particles can provide bioactivity to a polymer substrate. Collagen is used as protein derived animals has been used as good for tissue affinity, but recently, there is some risk of bovine spongiform encephalopathy (BSE). There is very meaningful on biology safety that HAp-coated sample made only an artificial thing is created. That is to say, HAp-coated sample is very high valuable as a novel composite and superior biology safety.

## **Conclusions**

A novel composite consisting of nano-scaled HAp particles and PET through covalent linkage was synthesized. This synthetic method is simpler and more reasonable in terms of requiring only a two-step procedure for obtaining the HAp/PET composite. The cell adhesion test shows that the HAp/PET composite improves bioactivity of poly (ethylene



terephthalate) (PET) fabric the surface of which was modified with nano-sized Hydroxyapatite (HAp) crystals through covalent bonding was developed for a soft-tissue-compatible material. In order to make covalent bonding between the HAp crystal and the PET surface, poly(*g*-methacryloxypropyl triethoxysilane) [poly(MPTS)] was grafted on the PET surface treated by H<sub>2</sub>O<sub>2</sub>. The surface grafting of poly(MPTS) onto the PET was confirmed by the weight gaining and X-ray photoelectron spectroscopy. The chemical reaction between OH groups on the HAp crystals and ethoxysilyl groups on the PET was conducted at 80°C for 2 h in reduced pressure. It was confirmed that the HAp/PET composite was not toxic for endothelial cells (HUVEC), and HUVEC adhered more plentifully on HAp-coated PET compared to untreated PET and hydrolyzed poly(MPTS)-grafted PET after 4 h of incubation.

### **Acknowledgements**

This work was supported by a grant from the Ministry of Health, Labour and Welfare of Japan

## References

1. V. Midy, C.Rey, E. Bres and M.Dard, *J.Biomed.Mater. Res.* 41 (1998) 405
2. M. Z. Paul, M. C. Catherine, B. C. Douglas and C. Y. A. Raymond, *ASAIO J.* 40 (1994) M896.
3. T.Furuzono, K.Sonoda and J. Tanaka, *J. Biomed. Mater. Res.* 56 (2001) 9.
4. T.Furuzono, P. L. Wang, A. Korematsu, K. Miyazaki, M. Oido-Mori, Y. Kowashi, K. Ohura, J. Tanaka and A. Kishida, *J. Biomed. Mater. Res.* 65B (2003) 217.
5. T. Furuzono, D. Walsh, K. Sato, K. Sonoda and J. Tanaka, *J Mater. Sci. Lett.* 20 (2001) 111.
6. K. Sonoda, T. furuzono, D. Walsh, K. Sato and J.Tanaka, *Solid State Ionics* 151 (2002) 327.
7. A Hebeish, S.E Shalaby, and A.M. Bayazeed, *J Appl Poly Sci* 26 (1981) 3245-3251
8. Stephane Poux and Sophie Demoustier-Champagne, *J Poly Sci* 41 (2003) 1347-1359
9. Tsutomu F, Shoji Y, Tsuyoshi K, Shingo K, Junzo T and Akio K, *J Artif Organs* 7 (2004) 137-144
10. Tsutomu F, Pao-Li Wang, Arata K, Kozo M, Mari Oido-Mori, Yusuke K, Kiyoshi O, Junzo T and Akio K,
11. S. P. Massia and J. A. Hubbell, *J Biomedical Materials Research* 25 (1991) 223-242
12. P. Hamerli, Th. Weigel, Th. Groth and D. Paul, *Biomaterials* 24 (2003) 3989-3999
13. T. Kawasaki, *J. Chromatogr.* 544 (1991) 147

**Table 1**  
**Elemental composition of deposited layers at different process parameters**  
**obtained by XPS**

Sample	C	O	Na	Si	Ca
Untreated PET	69.5	29.5	0.12	0.64	0.15
The poly (MPTS)-grafted PET	60.7	29.5	-	9.76	-

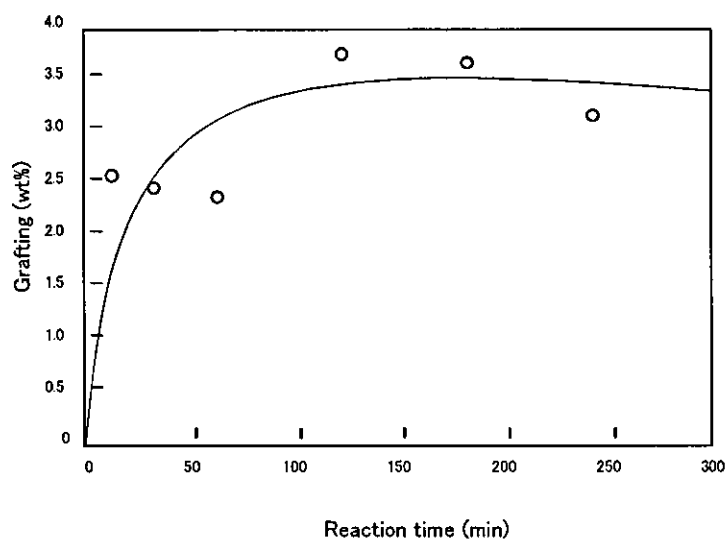


**Fig.1. Weight gain of poly(MPTRS)-grafted PET as a function of reaction time**

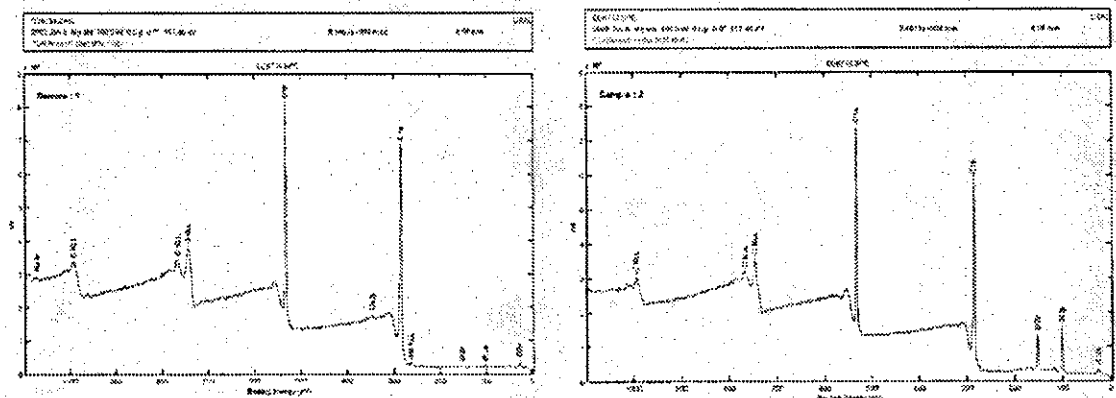


**Fig.2 Wide-scan spectra of a) the control surface and b) poly(MPTS) PET grafted at 85°C for 2 h**

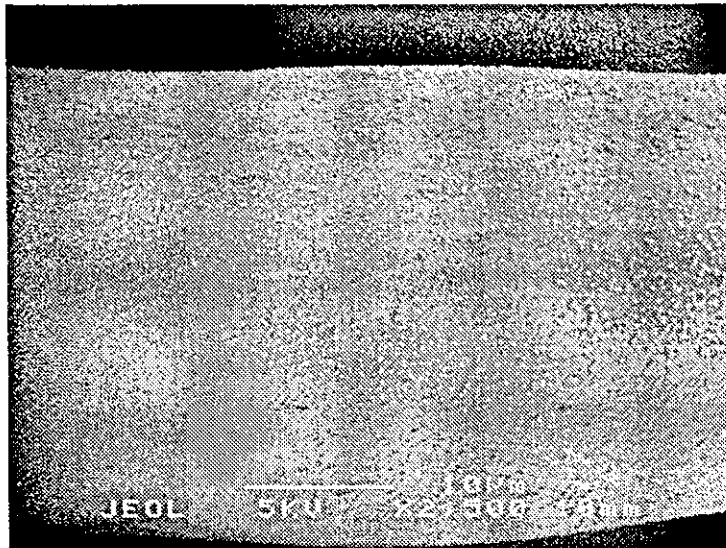


Fig.3. Scanning electron microscope (SEM) photograph of HAp particles covalently coated on a PET fiber

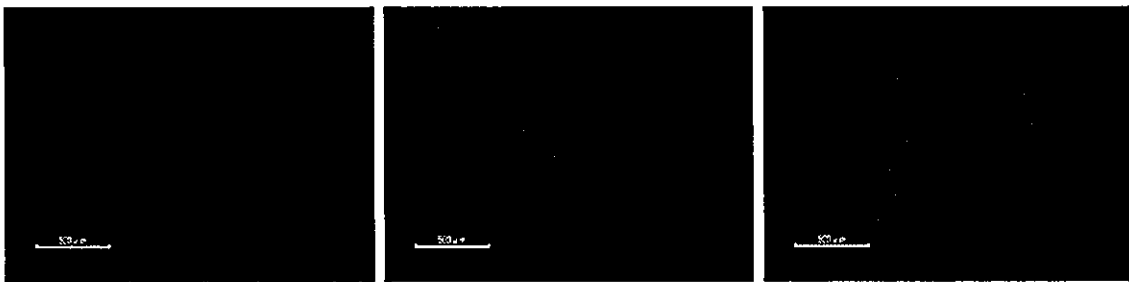


Figure 4. Fluorescent photographs of HUVEC cultured on three Culture substrates: HAp/PET composite, the original PET, and 5% collagen-coated PET, for 4 h. cell nuclei were stained with Hoechst 33342. Bar indicate 500µm.